Kir6.1 improves cardiac dysfunction in diabetic cardiomyopathy via the AKT-Foxo1 signaling pathway

Jinxin Wang
Chinese PLA General Hospital https://orcid.org/0000-0002-2906-0504

Jing Bai
Chinese PLA General Hospital

Peng Duan
Chinese PLA No. 371 hospital

Hao Wang
Chinese PLA General Hospital

Yang Li
Chinese PLA General Hospital

Qinglei Zhu (qlzhu@yahoo.com)
Chinese PLA General Hospital https://orcid.org/0000-0002-9582-4111

Original investigation

Keywords: Diabetic cardiomyopathy, Kir6.1, AKT, Foxo1, Cardiac dysfunction

Posted Date: June 5th, 2020

DOI: https://doi.org/10.21203/rs.3.rs-33214/v1

Abstract

Background: Diabetic cardiomyopathy (DCM) severely impairs the health of diabetic patients. Previous studies have shown that the expression of inwardly rectifying potassium channel 6.1 (Kir6.1) in heart mitochondria is significantly reduced in type 1 diabetes. However, whether its expression and function are changed and what role it plays in type 2 DCM have not been reported. This study investigated the role and mechanism of Kir6.1 in DCM.

Methods: The cardiac function in mice was analyzed by echocardiography, ELISA, hematoxylin and eosin staining, TUNEL and transmission electron microscopy. The mitochondrial function in cardiomyocytes was measured by the oxygen consumption rate and the mitochondrial membrane potential (ΔΨm). Kir6.1 expression at the mRNA and protein levels was analyzed by quantitative real-time PCR and western blotting (WB), respectively. The protein expression of t-AKT, p-AKT, t-Foxo1, and p-Foxo1 was analyzed by WB.

Results: We found that the cardiac function and the Kir6.1 expression in DCM mice were decreased. Kir6.1 overexpression improved cardiac dysfunction and upregulated the phosphorylation of AKT and Foxo1 in the DCM mouse model. Furthermore, Kir6.1 overexpression also improved cardiomyocyte dysfunction and upregulated the phosphorylation of AKT and Foxo1 in cardiomyocytes with insulin resistance. In contrast, cardiac-specific Kir6.1 knockout aggravated the cardiac dysfunction and downregulated the phosphorylation of AKT and Foxo1 in DCM mice. Furthermore, Foxo1 activation downregulated the expression of Kir6.1 and decreased the ΔΨm in cardiomyocytes. In contrast, Foxo1 inactivation upregulated the expression of Kir6.1 and increased the ΔΨm in cardiomyocytes. Chromatin immunoprecipitation assay demonstrated that the Kir6.1 promoter region contains a functional Foxo1-binding site .

Conclusions: Kir6.1 improves cardiac dysfunction in DCM, probably through the AKT-Foxo1 signaling pathway. Moreover, the crosstalk between Kir6.1 and the AKT-Foxo1 signaling pathway may provide new strategies for reversing the defective signaling in DCM.

Introduction

Diabetic cardiomyopathy (DCM), characterized by structural, morphological, functional, and metabolic abnormalities in the heart, severely impairs the health of diabetic patients and often occurs independently of myocardial ischemia, congenital heart disease, hypertension, and other cardiovascular diseases. Numerous molecular mechanisms have been proposed to contribute to the development of DCM, including altered myocardial insulin signaling, mitochondrial dysfunction, increased oxidative stress, autophagy, and dysregulation of Ca^{2+} handling [1], which result in cardiomyocyte necrosis, cardiac remodeling, and both diastolic and systolic dysfunction. Among these, altered myocardial insulin signaling may be the most common feature linking diabetes-induced alterations to the development of cardiac dysfunction [2].

Our previous studies have found that prolonged high-fat diet (HFD) feeding of animal models impairs protein kinase B (AKT) activation and forkhead box protein O1 (Foxo1) transcription factor phosphorylation, resulting in persistent Foxo1 nuclear localization and activation [3, 4]. Our recent study showed that persistently high insulin levels result in a significant decrease in the expression of phosphorylated AKT (p-AKT) and Foxo1 (p-Foxo1), mitochondrial membrane potential ($\Delta\Psi m$), and cardiac function in *db/db* mice, which indicates the links between altered insulin signaling and mitochondria in DCM [5].

ATP-sensitive potassium channel (K_{ATP}) plays an important protective role in the heart through various signaling pathways. K_{ATP} activation protects cardiomyocytes during heart failure, decreases ischemia/reperfusion injury, and reduces the occurrence of arrhythmias [6]. K_{ATP} is composed of two types of subunits, inwardly rectifying potassium channels and sulfonylurea receptors, and its subunit composition is tissue specific [7, 8]. There is a K_{ATP} channel in the inner membrane of mitochondria ($mitoK_{ATP}$). Inwardly rectifying potassium channel 6.1 (Kir6.1) is an important part of $mitoK_{ATP}$ channels in cardiomyocytes. A previous study has shown that the expression of Kir6.1 in heart mitochondria is significantly reduced in the mouse model of type 1 diabetes [9]. However, it has not been reported whether its expression and function are changed and what role it plays in type 2 DCM.

Therefore, we investigated the role and mechanism of Kir6.1 in type 2 DCM. By overexpressing and knocking out Kir6.1 in the mouse heart, we investigated the effect of Kir6.1 on cardiac function and on the expression of the AKT-Foxo1 signaling pathway in DCM. Furthermore, using primary ventricular cardiomyocyte cultures, we studied the effect of the AKT-Foxo1 signaling pathway on the expression of Kir6.1 and on the function of cardiomyocyte mitochondria.

Materials And Methods

Animal preparation and DCM model

Male pathogen-free C57BL/6J mice at 5 weeks of age were supplied by the Experimental Animal Center of PLA General Hospital. The study protocols were approved by the Ethics Committee of Chinese PLA General Hospital. All the mice were treated in strict accordance with the Guidelines for the Care and Use of Laboratory Animals. DCM was induced by sustained HFD (Research Diets, New Brunswick, NJ, USA) and single intraperitoneal injection of streptozotocin (STZ, Sigma-Aldrich, St. Louis, MO, USA) [10]. The mice were randomly divided into two groups: the DCM group was fed an HFD for 4 weeks, injected with STZ (100 μg/g of body weight), and then fed with HFD for another 12 weeks; the control group was fed a regular diet and injected with the same volume of vehicle (0.1 mol/L sodium citrate, Sigma-Aldrich). Plasma glucose levels were measured at the beginning and 12 weeks after the STZ injection by a Contour glucose meter (Roche, Basel, Switzerland). Mice with a fasting plasma glucose of over 13.89 mmol/L were considered diabetic. The diabetic mice were subjected to subsequent experiments.

Primary cardiomyocyte isolation and cell culture

Primary cultures of neonatal rat ventricular cardiomyocytes (NRVMs) were prepared from hearts of 1–2-day-old Sprague Dawley rats, as previously described [5]. NRVMs were cultured in Dulbecco's modified Eagle medium (DMEM) containing serum for 48 h.

Viral vector construction and transduction

A recombinant adeno-associated virus serotype 9 containing Kir6.1 (AAV-9) and a recombinant adenovirus encoding Kir6.1 (Ad-Kir6.1) were packaged by Shanghai HanBio Company (Shanghai, China). The AAV-9 capsid has previously been reported to show a modest preference for cardiac tissue *in vivo* [11]. The mice were randomized into two groups and injected with the null control virus (AAV-C) or AAV-9 via the tail vein before being fed standard rodent chow or an HFD. For the *in vitro* experiments, after 48 h of cell culture, the medium was changed with fresh DMEM containing serum and NRVMs were transfected by adding adenoviruses expressing green fluorescent protein (Ad-GFP) or GFP-fused Kir6.1 (Ad-Kir6.1). The adenovirus dose is indicated as multiplicity of infection (MOI). After 8 h of infection, the medium was changed to fresh DMEM containing serum for another 8 h of culturing, and then the cells were serum starved for 8 h. Then, insulin (100 nmol/L, 24 h; Sigma-Aldrich) was used to induce insulin resistance. Cells in the control group were treated with 100 nmol/L insulin for 0.5 h.

Echocardiography

Transthoracic two-dimensional M-mode echocardiography was performed on anesthetized mice using Vevo770 (VisualSonics, Toronto, Canada) equipped with a 30-MHz transducer. Left ventricular dimensions were measured according to the American Society for Echocardiography leading-edge method from at least three consecutive cardiac cycles. The echocardiography parameters included cardiac output (CO), ratio of mitral valve E velocity to A velocity (MV E/A), left ventricular ejection fraction (LVEF), left ventricular fractional shortening (LVFS), left ventricular posterior wall thickness at systole/diastole (LVPW; s/d), and left ventricular internal dimension at systole/diastole (LVID; s/d).

Brain natriuretic peptide measurement

Mouse serum samples and culture supernatants of cells were analyzed for brain natriuretic peptide (BNP) using commercial enzyme-linked immunosorbent assay (ELISA) kits (Ray Biotech, Norcross, GA, USA) according to the manufacturer's instructions.

Histological analysis

Hearts were fixed in 4% paraformaldehyde solution, embedded in paraffin, and sectioned (5 μm thickness). After dehydration, sections were stained with hematoxylin and eosin (H&E), and then viewed under a microscope (Olympus, Tokyo, Japan). For quantification, cell area measurements were performed on similar sections, and 20 nucleated cells were randomly selected to measure the mean cell area.

Apoptosis analysis

Hearts were fixed in 10% paraformaldehyde and embedded in paraffin. Paraffin-embedded sections were incubated at 60 °C for 15 min, dewaxed, and rehydrated. Heart tissue sections (5-μm thick) were used for

apoptosis detection with a TUNEL assay kit (Roche), as previously described [4].

Transmission electron microscopy

Hearts were fixed in 2.5% glutaraldehyde overnight, followed by osmication and uranyl acetate staining, dehydration in alcohol, and embedding in epoxy resin (Solarbio Life Science, Beijing, China). Ultrathin sections were stained with uranyl acetate and lead citrate (Sigma-Aldrich). The sections were viewed and imaged under a transmission electron microscope (Hitachi, Tokyo, Japan).

RNA isolation and quantitative real-time PCR analysis

RNA from heart tissue or NRVMs was extracted with TRIzol reagent (Invitrogen, Carlsbad, CA, USA). cDNA synthesis was performed with a PrimeScript™ RT regent Kit (Takara, Kyoto, Japan). Quantitative real-time PCR (qRT-PCR) was performed in duplicate in a total reaction volume of 25 μL using SYBR-Green master mix (Takara) and conventional protocols. The primer sequences for qRT-PCR are listed in Supplementary Table 1. Expression was normalized to that of the housekeeping gene, *36β4*. Quantitative data was calculated using the comparative CT method.

Protein analysis by western blotting

Proteins from tissues or cell cultures were extracted and resolved by SDS-PAGE, and transferred to nitrocellulose membranes for immunoblotting analysis, using specific antibodies (Abcam, Cambridge, MA, USA). The signal intensity was measured and analyzed by Image J software, as previously described [3]. The expression of specific proteins was normalized to the protein expression of GAPDH.

Oxygen consumption rate measurement

A Seahorse Bioscience XFe96 extracellular flux analyzer was used to measure the oxygen consumption rate (OCR) in NRVMs using a previously reported protocol [12]. NRVMs were plated at 3000 cells per well in XF media supplemented with pyruvate (1 mM), glutamine (2 mM), and glucose (10 mM; Sigma-Aldrich). Four independent OCR measurements were taken for each condition: baseline, and following the addition of oligomycin (1 μM), FCCP (2 μM), and antimycin A (0.5 μM) plus rotenone (0.5 μM; Agilent, Santa Clara, CA, USA). The protein concentration of NRVMs was determined for each well using a standard Bradford assay. Data were analyzed by the Wave software and Report generator.

Generation of cardiac-specific Kir6.1-knockout mice

Kir6.1$^{lox/lox}$ mice and MerCreMer mice (C57BL/6J background) were purchased from Guangzhou Cyagen Company (Guangzhou, China). Kir6.1$^{lox/lox}$ mice were crossed with MerCreMer mice to generate cardiac-specific *Kir6.1*-knockout (Kir6.1$^{lox/lox}$/MerCreMer, KO) mice. The Cre-mediated excision of the Kir6.1 floxed-allele in the heart was induced by daily intraperitoneal tamoxifen (20 mg/kg/day; Sigma-Aldrich) injections for five consecutive days. Two days later, the KO&DCM group was fed an HFD for 4 weeks, injected with STZ (100 μg/g of body weight), and then fed with HFD for another 12 weeks; the control

group was fed a regular diet and injected with the same volume of vehicle (0.1 mol/L sodium citrate). Littermate Kir6.1$^{wt/lox}$/MerCreMer mice were used as controls.

Mitochondrial membrane potential measurement

After 48 h of cell culture, NRVMs were divided into three groups: control, MK-2206 dihydrochloride (5 μmol/L, 0.5 h, Selleck Chemicals, Houston, TX, USA) plus insulin (100 nmol/L, 3 h; MK-2206&INS), and insulin (100 nmol/L, 3 h; INS). Transitory insulin stimulation activates AKT and thereby inactivates Foxo1. MK-2206 dihydrochloride (MK-2206) is an AKT inhibitor, AKT inhibition activates Foxo1 [3, 4]. The ΔΨm of NRVMs was measured using the fluorescent dye, JC-1 (Beyotime Biotechnology, Shanghai, China) as described previously [5]. The images were analyzed by Image Pro Plus 6.0 software. The ΔΨm was determined by calculating the ratio of red fluorescence to green fluorescence.

Chromatin immunoprecipitation assay

Chromatin immunoprecipitation assay was performed as described previously [3, 13]. Heart chromatin was isolated from mice by immunoprecipitation with anti-Foxo1 antibodies or control IgG. Occupancy of the Foxo1 site in the *Kir6.1* promoter was determined by PCR; control immunoprecipitation with nonrelevant IgG demonstrated the specificity of the assay. The primer sequences for PCR: 5'-CCGTCCTGCTGGGTGTAAAT-3' and 5'-ATATAGAGGGGTGGGAGGGC-3'.

Statistical Analysis

Statistical analysis was performed with SPSS 17.0 software. Data are expressed as the mean ± SEM. Comparisons of parameters between two groups were performed with unpaired Student's *t*-test. Comparisons of parameters among groups were determined by one-way ANOVA, followed by the Scheffe multiple comparison test. $P < 0.05$ was considered statistically significant.

Results

Cardiac and mitochondrial function are decreased in DCM mice and in insulin-resistant NRVMs

The cardiac function of DCM and control mice was analyzed by echocardiography. Compared with the control mice, the DCM mice showed a significant reduction in CO, MV E/A, LVEF, LVFS, and LVPW; d, and an increase in LVID; d/s, thereby exhibiting DCM (Fig. 1A). ELISA demonstrated that the BNP protein expression was significantly increased in the heart of diabetic mice (Fig. 1B). The myocardial structure was examined by H&E staining. Diabetic hearts displayed structural abnormalities, including abnormal cellular structures, the existence of foci with necrotic myocytes, and increased cardiomyocyte areas (Fig. 1C). The TUNEL assay was performed to examine apoptosis of cardiomyocytes. The proportion of apoptotic cells was remarkably increased in diabetic hearts compared with the controls (Fig. 1D). We further examined the cardiac ultrastructure by transmission electron microscopy. Well-organized morphology of sarcomeres, mitochondria, and Z-line was observed in the control hearts. However,

diabetic hearts exhibited enlarged sarcomeres and abnormal changes in mitochondrial structure, including irregular arrangement, swelling, and vacuolated and disrupted cristae (Fig. 1E). These results indicated the successful establishment of the *in vivo* HFD&STZ-induced DCM mouse model.

Subsequently, NRVMs were treated with insulin to induce the cardiomyocyte model of insulin resistance. The level of BNP in the culture supernatant was increased in chronic insulin-treated NRVMs (Fig. 1F). We further measured the OCR in cardiomyocytes by a Seahorse XFe96 Analyzer. Chronic insulin stimulation significantly decreased the OCR, as manifested by basal respiration, ATP production, maximal respiration, and spare respiratory capacity (Fig. 1G).

The expression of Kir6.1 is decreased in HFD&STZ-induced type 2 diabetic mice and in chronic insulin-resistant NRVMs

qRT-PCR analysis indicated that the *Kir6.1* mRNA expression was significantly decreased in DCM hearts (Fig. 2A). Western blot analysis confirmed that Kir6.1 protein expression was reduced by 40% in DCM mice compared with the control mice (Fig. 2B).

In accordance with the *in vivo* results, the mRNA and protein levels of Kir6.1 in NRVMs were obviously decreased after chronic insulin stimulation (Fig. 2C and D). These results imply that Kir6.1 expression decreases with the decrease in cardiac function, suggesting it may play a special role in DCM.

Kir6.1 overexpression improves cardiac dysfunction in DCM mice and in insulin-resistant NRVMs

Kir6.1 expression was confirmed by western blotting. The mice infected with AAV-9 exhibited higher protein levels of Kir6.1 by about 1.3-fold compared with the control (Fig. 3A). To evaluate the efficacy of the *Kir6.1* gene transfection, NRVMs were transfected with Ad-GFP at different MOIs (30, 50, 80, and 100). The best transfection efficiency was detected in the cells transfected with Ad-GFP at an MOI of 80 (Supplementary Fig. 1). The NRVMs transfected with Ad-Kir6.1 showed upregulated Kir6.1 protein expression compared with the cells transfected with the control adenovirus (Fig. 3B).

The echocardiography data showed the protective effects of Kir6.1 on the HFD&STZ-induced decrease in CO, LVEF, and LVFS (Fig. 3C). Kir6.1 overexpression obviously suppressed the BNP protein level in the DCM mice (Fig. 3D). It also alleviated HFD&STZ-induced cardiomyocyte injury. The inhibitory effects of Kir6.1 on cardiac hypertrophy were further confirmed by the quantitative measurements of the cardiomyocyte area determined by H&E staining (Fig. 3E). Furthermore, Kir6.1 overexpression significantly reduced diabetes-induced myocardial cell apoptosis (Fig. 3F) and rescued the myocardial morphology in DCM mice (Fig. 3G).

Kir6.1 overexpression in chronic insulin-stimulated NRVMs significantly decreased the level of BNP in the culture supernatant (Fig. 3H). Furthermore, this overexpression attenuated the mitochondrial respiration

dysfunction in chronic insulin-stimulated NRVMs, including basal respiration, ATP production, maximal respiration, and spare respiratory capacity (Fig. 3I).

Cardiac-specific Kir6.1 knockout aggravates cardiac dysfunction in diabetic mice

We used cardiac-specific *Kir6.1*-knockout mice to further study the role of Kir6.1 in DCM. qRT-PCR and western blotting confirmed that the mRNA and protein levels of Kir6.1 in the heart of KO mice were significantly decreased compared with those in the control mice (Fig. 4A and B).

Kir6.1 deficiency increased the deterioration in cardiac function induced by HFD&STZ, as manifested by the increase in LVID; d and the reduction in CO, LVEF, and LVPW; d (Fig. 4C). Kir6.1 deficiency in the heart resulted in higher BNP protein level in DCM mice compared with the control mice (Fig. 4D). Cardiac-specific Kir6.1 knockout also aggravated cardiac pathological changes in DCM mice, as demonstrated by the quantitative data of cardiomyocyte area determined by H&E staining (Fig. 4E). Furthermore, the apoptosis rate in cardiac-specific *Kir6.1*-knockout DCM mice was significantly increased compared with that in DCM mice (Fig. 4F). Moreover, Kir6.1 knockout exacerbated the myocardial morphology in DCM mice (Fig. 4G).

Effect of Kir6.1 on the AKT-Foxo1 signaling pathway in DCM

To understand the mechanism by which Kir6.1 overexpression reduces cardiac dysfunction in DCM, the changes in the AKT-Foxo1 signaling pathway were investigated *in vivo* and *in vitro*. The expression of p-AKT and p-Foxo1 was markedly downregulated in the DCM group and Insulin group. Kir6.1 knockout further decreased the phosphorylation of AKT and Foxo1 in DCM mice (Fig. 5A). However, Kir6.1 overexpression increased the levels of p-AKT and p-Foxo1 in DCM mice (Fig. 5B). Consistent with the *in vivo* results, the levels of p-AKT and p-Foxo1 were upregulated in the Ad-Kir6.1&Insulin-treated NRVMs (Fig. 5C). These findings demonstrated that Kir6.1 overexpression attenuates cardiac dysfunction in DCM, probably through the AKT-Foxo1 signaling pathway.

Effect of the AKT-Foxo1 signaling pathway on the expression of Kir6.1 and the function of mitochondria in cardiomyocytes

We next examined the role of the AKT-Foxo1 signaling pathway in regulating Kir6.1 expression and mitochondrial function in cardiomyocytes. The expression of p-AKT, p-Foxo1, and Kir6.1 was markedly decreased in the MK-2206&INS group (Fig. 6A). In contrast, the expression of p-AKT, p-Foxo1, and Kir6.1 in the INS group was increased compared with the MK-2206&INS group (Fig. 6A).

In the MK-2206&INS group, the ΔΨm was lower than that in the control group. However, in the INS group it was higher than that in the MK-2206&INS group (Fig. 6B and C).

Finally, we examined whether the promoter region of *Kir6.1* has a consensus Foxo1-binding site. A region of 2.0 kb in the mouse *Kir6.1* promoter was analyzed with the Jaspar genome database and three consecutive copies of the conserved Foxo1-binding sequence were identified (Fig. 6D). To determine whether Foxo1 interacts with this promoter region, chromatin immunoprecipitation experiments were performed, which indicated that endogenous Foxo1 interacted with the consensus DNA sequence in the *Kir6.1* promoter region (Fig. 6E).

Discussion

In this study, we investigated the role and mechanism of Kir6.1 in DCM. We found that the cardiac function and Kir6.1 expression were decreased in DCM mice. Kir6.1 overexpression improved cardiac dysfunction and upregulated the phosphorylation of AKT and Foxo1 in DCM, both *in vivo* and *in vitro*. In contrast, cardiac-specific Kir6.1 knockout aggravated the cardiac dysfunction and downregulated the phosphorylation of AKT and Foxo1 in DCM mice. Activation of Foxo1 downregulated the expression of Kir6.1 and decreased the ΔΨm in cardiomyocytes. In contrast, inactivation of Foxo1 upregulated the expression of Kir6.1 and increased the ΔΨm in cardiomyocytes. Furthermore, Foxo1 was shown to interact with the promoter region of *Kir6.1* for transcription activation.

Diabetic cardiomyopathy is becoming a well-known clinical phenomenon. The metabolic milieu associated with diabetes, such as hyperglycemia and hyperinsulinemia, alters multiple molecular pathways within the cardiomyocyte, thereby impairing cardiac contractility and promoting myocyte dysfunction, injury, and cell death [1]. Systolic and diastolic dysfunction can be consistently reproduced in a variety of rodent models of diabetes. Echocardiography is a standard modality for diagnosing DCM. There are three myocardial signals in DCM: left ventricular (LV) diastolic dysfunction, abnormal LV systolic function, and changes in LV geometry [14]. Alteration in the BNP level suggests myocardial structural and functional dysfunction. Elevated BNP levels showed a positive correlation with LV dysfunction in DCM [15]. Cardiomyocyte hypertrophy is a common structural hallmark in patients with DCM [16, 17]. A relatively oxygen-poor environment induced by hypertrophy accelerates cardiomyocyte apoptosis. Cardiac function is energetically demanding, and thus reliant on efficient well-coupled mitochondria to generate adenosine triphosphate (ATP). Extensive experimental results demonstrated that cardiomyocytes from animal models of type 1 and 2 diabetes had altered mitochondrial morphology and mitochondrial dysfunction [18].

The mitoK_{ATP} subunit, Kir6.1, plays a major role in maintaining mitochondrial function. Alteration in mitochondrial function has been linked to cardiovascular diseases including DCM [19, 20]. Furthermore, numerous studies have shown the cardioprotective roles of mitoK_{ATP} [21]. In our study, the expression of Kir6.1 was decreased in the mouse model of type 2 DCM. In accordance with the *in vivo* results, it was decreased in a cardiomyocyte model of insulin resistance, which was also consistent with a previous

study [9]. The data indicated that Kir6.1 may play a special role in DCM. Therefore, transgenic mice overexpressing Kir6.1 or lacking Kir6.1 specifically in the heart were used to study the role of Kir6.1 in DCM. Previous studies have shown that AAV-9 leads to preferential cardiac transduction *in vivo* [11, 22]. Moreover, cardiomyocytes can be efficiently transfected by adenoviruses. Our data showed that Kir6.1 expression was overexpressed *in vivo* and *in vitro* after AAV-9 or adenoviral gene transfer, respectively. The ability to control the tissue specificity of gene knockout in the rodent using the Cre-loxP technology has profoundly advanced rodent genetics and the ability to examine single gene functions *in vivo* [23]. We used the Cre-loxP technology to modify gene expression in our mouse model. The expression of Kir6.1 in the heart was significantly decreased after intraperitoneal tamoxifen injection, indicating that the cardiac-specific *Kir6.1*-knockout mouse model was successfully established.

In this study, we found that the cardiac function in DCM mice was decreased, including systolic and diastolic dysfunction, increase in BNP, cardiomyocyte hypertrophy and apoptosis, and abnormal changes in mitochondrial structure *in vivo*. Additionally, we found increased BNP levels and reduction in the OCR *in vitro*. DCM and its associated mitochondrial dysfunction have been observed in *ob/ob*, *db/db* and HFD-fed mice [24, 25]. Furthermore, cardiac tissue from Akita mice displayed swollen mitochondria, lacking a well-defined cristae structure along with decreased states 3 and 4 respiration and ATP synthesis [26]. Our data agree with many previous studies on cardiac dysfunction in rodent models of DCM [27–31]. However, in the current study, Kir6.1 overexpression reduced cardiac dysfunction in diabetic mice and dysfunction of cardiomyocytes with insulin resistance, whereas cardiac-specific Kir6.1 knockout aggravated cardiac dysfunction in diabetic mice. Thus, our findings suggest that Kir6.1 overexpression attenuates cardiac dysfunction in DCM.

Cardiac insulin signaling mediates cellular homeostasis by controlling substrate use, protein synthesis, autophagy, and cell survival [32]. Physiologically, binding of insulin to insulin receptor (IR) activates insulin receptor substrate 1 and 2 (IRS1 and IRS2) and the downstream phosphoinositide 3-kinase (PI3K)-AKT pathways. AKT is required for cardiac growth, metabolism, and survival, and its targets include p70S6K (protein synthesis), Glut4 (glucose transport), and Foxo1 (gene expression) [33]. Briefly, insulin exerts its function through AKT activation, which in turn phosphorylates Foxo1. In cardiomyocytes, Foxo1 is involved in the control of many important properties such as cell growth, metabolic adaptation, cell apoptosis, autophagy, and resistance to oxidative stress [34, 35]. Impaired glucose uptake in the diabetic heart is often linked with reduced expression or activity of the downstream intermediates in the insulin signaling pathway. In this study, the levels of p-AKT and p-Foxo1 were markedly downregulated in DCM. Decreased cardiac basal and insulin-stimulated phosphorylation of AKT and Foxo1 is evident in diabetic mouse models [36]. In our previous studies, prolonged HFD feeding of mouse models impaired AKT activation and Foxo1 phosphorylation, which resulted in persistent Foxo1 nuclear localization and activation [3, 4], consequently leading to cardiac dysfunction. Furthermore, our recent study showed a reduction in the expression of p-AKT and p-Foxo1 and in cardiac function in *db/db* mice [5]. K_{ATP} plays a key protective role in the heart through various signaling pathways. Specifically, genetic manipulation of cardiomyocyte insulin signaling intermediates has demonstrated that partial cardiac function rescue was

achieved by upregulation of the insulin signaling pathway in diabetic hearts [37]. Similarly, a previous study has reported that the cardioprotective effect of K_{ATP} occurs at least partially by regulating the AKT-Foxo1 signaling pathway, which in turn influences the expression of PGC-1α and its downstream target genes [38]. Our recent study also showed that opening of mitoK_{ATP} increased the phosphorylation of AKT and Foxo1, but the effects of this opening were blocked by the specific AKT inhibitor, MK-2206 [5]. In our current study, Kir6.1 knockout further suppressed the phosphorylation of AKT and Foxo1 in DCM mice and increased cardiac dysfunction. On the contrary, Kir6.1 overexpression upregulated the phosphorylation of AKT and Foxo1 in DCM models and improved cardiac dysfunction both *in vivo* and *in vitro*. The above data indicate that Kir6.1 overexpression attenuates cardiac dysfunction in DCM, probably through the AKT-Foxo1 signaling pathway.

Foxo1 and its downstream targets play a key role in mitochondrial biogenesis [39]. Transient insulin stimulation activates the PI3K-AKT signaling pathway and suppresses Foxo1 activation. Inactivation of AKT through an AKT-specific inhibitor activated Foxo1. Activation of Foxo1 results in heme deficiency, limiting mitochondrial cofactor biosynthesis and ATP production [3, 4, 40]. The stability of ΔΨm is important for energy conversion. A decrease in the ΔΨm affects energy conversion, leading to cell dysfunction [41]. In our study, the AKT-specific inhibitor, MK-2206, prevented endogenous AKT activation, resulting in Foxo1 activation, decreased Kir6.1 expression and reduced ΔΨm. However, Foxo1 inactivation upregulated Kir6.1 expression and increased ΔΨm. Foxo1 promotes loss of mitochondria by activating the gene expression of hemeoxygenase-1, an enzyme that catalyzes heme degradation. Heme is an essential component of mitochondrial complexes III and IV [3, 40]. Chromatin immunoprecipitation assay demonstrated that the *Kir6.1* promoter region contains a functional Foxo1-binding site. Foxo1 interacts with the promoter region of Kir6.1 for transcriptional activation. Our results indicate that the interaction between the AKT-Foxo1 signaling pathway and Kir6.1 may play a key role in the pathogenesis of DCM.

Conclusions

In conclusion, our results provided *in vivo* and *in vitro* evidence that Kir6.1 improves cardiac dysfunction in DCM, probably through the AKT-Foxo1 signaling pathway. Moreover, the crosstalk between Kir6.1 and the AKT-Foxo1 signaling pathway may provide new strategies for reversing the defective signaling in DCM.

Additional File

Additional file 1. Additional figures and tables.

Abbreviations

DCM: Diabetic cardiomyopathy; HFD: high-fat diet; AKT: protein kinase B; Foxo1: forkhead box protein O1; ΔΨm: mitochondrial membrane potential; K_{ATP}: ATP-sensitive potassium channel; mitoK_{ATP}: K_{ATP} channel in the inner membrane of mitochondria; Kir6.1: inwardly rectifying potassium channel 6.1; STZ:

streptozotocin; NRVMs: neonatal rat ventricular cardiomyocytes; AAV-9: recombinant adeno-associated virus serotype 9; Ad-Kir6.1: recombinant adenovirus encoding Kir6.1; OCR: oxygen consumption rate.

Declarations

Author's contributions

WJX designed the study, analyzed and interpreted the data, and drafted the paper. BJ and DP contributed to data acquisition. WH and LY analyzed and interpreted the data. ZQL designed the study and drafted the paper. All authors read and approved the final manuscript.

Author details

[1]Department of Cardiology, Chinese PLA General Hospital, Beijing 100853, China

[2]Department of Geriatric Cardiology, Chinese PLA General Hospital, National Clinical Research Center for Geriatric Diseases, Beijing 100853, China

[3]Department of Cardiology, Chinese PLA No. 371 Hospital, Henan 453000, China

Acknowledgements

Not applicable.

Competing interests

The authors declare that they have no competing interests.

Availability of data and materials

The datasets used and/or analyzed during the current study are available from the corresponding author on reasonable request.

Consent for publication

Not applicable.

Ethics approval and consent to participate

The study was approved by the Ethics Committee of Chinese PLA General Hospital.

Funding

This work was supported by the National Natural Science Foundation of China [grant numbers 81570349 and 81200157].

References

1. Bugger H, Abel ED. Molecular mechanisms of diabetic cardiomyopathy. Diabetologia. 2014;57(4):660–71.
2. Riehle C, Bauersachs J. Of mice and men: models and mechanisms of diabetic cardiomyopathy. Basic Res Cardiol. 2018;114(1):2.
3. Qi Y, Zhu Q, Zhang K, Thomas C, Wu Y, Kumar R, Baker KM, Xu Z, Chen S, Guo S. Activation of Foxo1 by insulin resistance promotes cardiac dysfunction and beta-myosin heavy chain gene expression. Circ Heart Fail. 2015;8(1):198–208.
4. Qi Y, Xu Z, Zhu Q, Thomas C, Kumar R, Feng H, Dostal DE, White MF, Baker KM, Guo S. Myocardial loss of IRS1 and IRS2 causes heart failure and is controlled by p38alpha MAPK during insulin resistance. Diabetes. 2013;62(11):3887–900.
5. Duan P, Wang J, Li Y, Wei S, Su F, Zhang S, Duan Y, Wang L, Zhu Q. Opening of mitoKATP improves cardiac function and inhibits apoptosis via the AKT-Foxo1 signaling pathway in diabetic cardiomyopathy. Int J Mol Med. 2018;42(5):2709–19.
6. Tinker A, Aziz Q, Thomas A. The role of ATP-sensitive potassium channels in cellular function and protection in the cardiovascular system. Br J Pharmacol. 2014;171(1):12–23.
7. Li N, Wu JX, Ding D, Cheng J, Gao N, Chen L. Structure of a Pancreatic ATP-Sensitive Potassium Channel. Cell. 2017;168(1–2):101–10.
8. Ye P, Zhu YR, Gu Y, Zhang DM, Chen SL. Functional protection against cardiac diseases depends on ATP-sensitive potassium channels. J Cell Mol Med. 2018;22(12):5801–6.
9. Fancher IS, Dick GM, Hollander JM. Diabetes mellitus reduces the function and expression of ATP-dependent K(+) channels in cardiac mitochondria. Life sciences. 2013;92(11):664–8.
10. Kusakabe T, Tanioka H, Ebihara K, Hirata M, Miyamoto L, Miyanaga F, Hige H, Aotani D, Fujisawa T, Masuzaki H, Hosoda K, Nakao K. Beneficial effects of leptin on glycaemic and lipid control in a mouse model of type 2 diabetes with increased adiposity induced by streptozotocin and a high-fat diet. Diabetologia. 2009;52(4):675–83.
11. Pacak CA, Mah CS, Thattaliyath BD, Conlon TJ, Lewis MA, Cloutier DE, Zolotukhin I, Tarantal AF, Byrne BJ. Recombinant adeno-associated virus serotype 9 leads to preferential cardiac transduction in vivo. Circulation research. 2006;99(4):e3–9.
12. Khan M, Nickoloff E, Abramova T, Johnson J, Verma SK, Krishnamurthy P, Mackie AR, Vaughan E, Garikipati VN, Benedict C, Ramirez V, Lambers E, Ito A, Gao E, Misener S, Luongo T, Elrod J, Qin G, Houser SR, Koch WJ, Kishore R. Embryonic stem cell-derived exosomes promote endogenous repair mechanisms and enhance cardiac function following myocardial infarction. Circulation research. 2015;117(1):52–64.
13. Qi Y, Zhang K, Wu Y, Xu Z, Yong QC, Kumar R, Baker KM, Zhu Q, Chen S, Guo S. Novel Mechanism of Blood Pressure Regulation By Forkhead Box Class O1–Mediated Transcriptional Control of Hepatic Angiotensinogen. Hypertension. 2014;64(5):1131–40.

14. Marwick TH, Ritchie R, Shaw JE, Kaye D. Implications of Underlying Mechanisms for the Recognition and Management of Diabetic Cardiomyopathy. J Am Coll Cardiol. 2018;71(3):339–51.
15. Murtaza G, Virk HUH, Khalid M, Lavie CJ, Ventura H, Mukherjee D, Ramu V, Bhogal S, Kumar G, Shanmugasundaram M, Paul TK. Diabetic cardiomyopathy - A comprehensive updated review. Prog Cardiovasc Dis. 2019;62(4):315–26.
16. Bernardo BC, Weeks KL, Pretorius L, McMullen JR. Molecular distinction between physiological and pathological cardiac hypertrophy: experimental findings and therapeutic strategies. Pharmacol Ther. 2010;128(1):191–227.
17. van Empel VP, De Windt LJ. Myocyte hypertrophy and apoptosis: a balancing act. Cardiovascular research. 2004;63(3):487–99.
18. Galloway CA, Yoon Y. Mitochondrial dynamics in diabetic cardiomyopathy. Antioxid Redox Signal. 2015;22(17):1545–62.
19. Westermeier F, Navarro-Marquez M, Lopez-Crisosto C, Bravo-Sagua R, Quiroga C, Bustamante M, Verdejo HE, Zalaquett R, Ibacache M, Parra V, Castro PF, Rothermel BA, Hill JA, Lavandero S. Defective insulin signaling and mitochondrial dynamics in diabetic cardiomyopathy. Biochim Biophys Acta. 2015;1853(5):1113–8.
20. Ong SB, Hall AR, Hausenloy DJ. Mitochondrial dynamics in cardiovascular health and disease. Antioxid Redox Signal. 2013;19(4):400–14.
21. Queliconi BB, Wojtovich AP, Nadtochiy SM, Kowaltowski AJ, Brookes PS. Redox regulation of the mitochondrial K(ATP) channel in cardioprotection. Biochim Biophys Acta. 2011;1813(7):1309–15.
22. Prasad KM, Xu Y, Yang Z, Acton ST, French BA. Robust cardiomyocyte-specific gene expression following systemic injection of AAV: in vivo gene delivery follows a Poisson distribution. Gene therapy. 2011;18(1):43–52.
23. Sohal DS, Nghiem M, Crackower MA, Witt SA, Kimball TR, Tymitz KM, Penninger JM, Molkentin JD. Temporally regulated and tissue-specific gene manipulations in the adult and embryonic heart using a tamoxifen-inducible Cre protein. Circulation research. 2001;89(1):20–5.
24. Boudina S, Sena S, O'Neill BT, Tathireddy P, Young ME, Abel ED. Reduced Mitochondrial Oxidative Capacity and Increased Mitochondrial Uncoupling Impair Myocardial Energetics in Obesity. Circulation. 2005;112(17):2686–95.
25. Dabkowski ER, Baseler WA, Williamson CL, Powell M, Razunguzwa TT, Frisbee JC, Hollander JM. Mitochondrial dysfunction in the type 2 diabetic heart is associated with alterations in spatially distinct mitochondrial proteomes. Am J Physiol Heart Circ Physiol. 2010;299(2):H529–40.
26. Bugger H, Chen D, Riehle C, Soto J, Theobald HA, Hu XX, Ganesan B, Weimer BC, Abel ED. Tissue-specific remodeling of the mitochondrial proteome in type 1 diabetic akita mice. Diabetes. 2009;58(9):1986–97.
27. Tsushima K, Bugger H, Wende AR, Soto J, Jenson GA, Tor AR, McGlauflin R, Kenny HC, Zhang Y, Souvenir R, Hu XX, Sloan CL, Pereira RO, Lira VA, Spitzer KW, Sharp TL, Shoghi KI, Sparagna GC, Rog-Zielinska EA, Kohl P, Khalimonchuk O, Schaffer JE. E.D. Abel, Mitochondrial Reactive Oxygen Species

in Lipotoxic Hearts Induce Post-Translational Modifications of AKAP121, DRP1, and OPA1 That Promote Mitochondrial Fission. Circulation research. 2018;122(1):58–73.

28. Waldman M, Cohen K, Yadin D, Nudelman V, Gorfil D, Laniado-Schwartzman M, Kornwoski R, Aravot D, Abraham NG, Arad M, Hochhauser E. Regulation of diabetic cardiomyopathy by caloric restriction is mediated by intracellular signaling pathways involving 'SIRT1 and PGC-1α'. Cardiovascular diabetology. 2018;17(1):111.
29. Liu L, Zhang X, Qian B, Min X, Gao X, Li C, Cheng Y, Huang J. Over-expression of heat shock protein 27 attenuates doxorubicin-induced cardiac dysfunction in mice. Eur J Heart Fail. 2007;9(8):762–9.
30. Zuo GF, Ren XM, Ge Q, Luo J, Ye P, Wang F, Wu W, Chao YL, Gu Y, Gao XF, Ge Z, Gao HB, Hu ZY, Zhang JJ, Chen SL. Activation of the PP2A catalytic subunit by ivabradine attenuates the development of diabetic cardiomyopathy. J Mol Cell Cardiol. 2019;130:170–83.
31. Zhang Y, Zhang YY, Li TT, Wang J, Jiang Y, Zhao Y, Jin XX, Xue GL, Yang Y, Zhang XF, Sun YY, Zhang ZR, Gao X, Du ZM, Lu YJ, Yang BF, Pan ZW. Ablation of interleukin-17 alleviated cardiac interstitial fibrosis and improved cardiac function via inhibiting long non-coding RNA-AK081284 in diabetic mice. J Mol Cell Cardiol. 2018;115:64–72.
32. Riehle C, Abel ED. Insulin Signaling and Heart Failure. Circulation research. 2016;118(7):1151–69.
33. Walsh K. Akt signaling and growth of the heart. Circulation. 2006;113(17):2032–4.
34. Battiprolu PK, Hojayev B, Jiang N, Wang ZV, Luo X, Iglewski M, Shelton JM, Gerard RD, Rothermel BA, Gillette TG, Lavandero S, Hill JA. Metabolic stress-induced activation of FoxO1 triggers diabetic cardiomyopathy in mice. J Clin Investig. 2012;122(3):1109–18.
35. Puthanveetil P, Wan A, Rodrigues B. FoxO1 is crucial for sustaining cardiomyocyte metabolism and cell survival. Cardiovascular research. 2013;97(3):393–403.
36. Shum M, Bellmann K, St-Pierre P, Marette A. Pharmacological inhibition of S6K1 increases glucose metabolism and Akt signalling in vitro and in diet-induced obese mice. Diabetologia. 2016;59(3):592–603.
37. Varma U, Koutsifeli P, Benson VL, Mellor KM, Delbridge LMD. Molecular mechanisms of cardiac pathology in diabetes – Experimental insights, Biochimica et Biophysica Acta (BBA) -. Molecular Basis of Disease. 2018;1864(5):1949–59.
38. Hu X, Xu X, Huang Y, Fassett J, Flagg TP, Zhang Y, Nichols CG, Bache RJ, Chen Y. Disruption of sarcolemmal ATP-sensitive potassium channel activity impairs the cardiac response to systolic overload. Circulation research. 2008;103(9):1009–17.
39. Wang P, Wang L, Lu J, Hu Y, Wang Q, Li Z, Cai S, Liang L, Guo K, Xie J, Wang J, Lan R, Shen J, Liu P. SESN2 protects against doxorubicin-induced cardiomyopathy via rescuing mitophagy and improving mitochondrial function. J Mol Cell Cardiol. 2019;133:125–37.
40. Cheng Z, Guo S, Copps K, Dong X, Kollipara R, Rodgers JT, Depinho RA, Puigserver P, White MF. Foxo1 integrates insulin signaling with mitochondrial function in the liver. Nature medicine. 2009;15(11):1307–11.

41. Brand MD, Nicholls DG. Assessing mitochondrial dysfunction in cells. Biochem J. 2011;435(2):297–312.

Figures

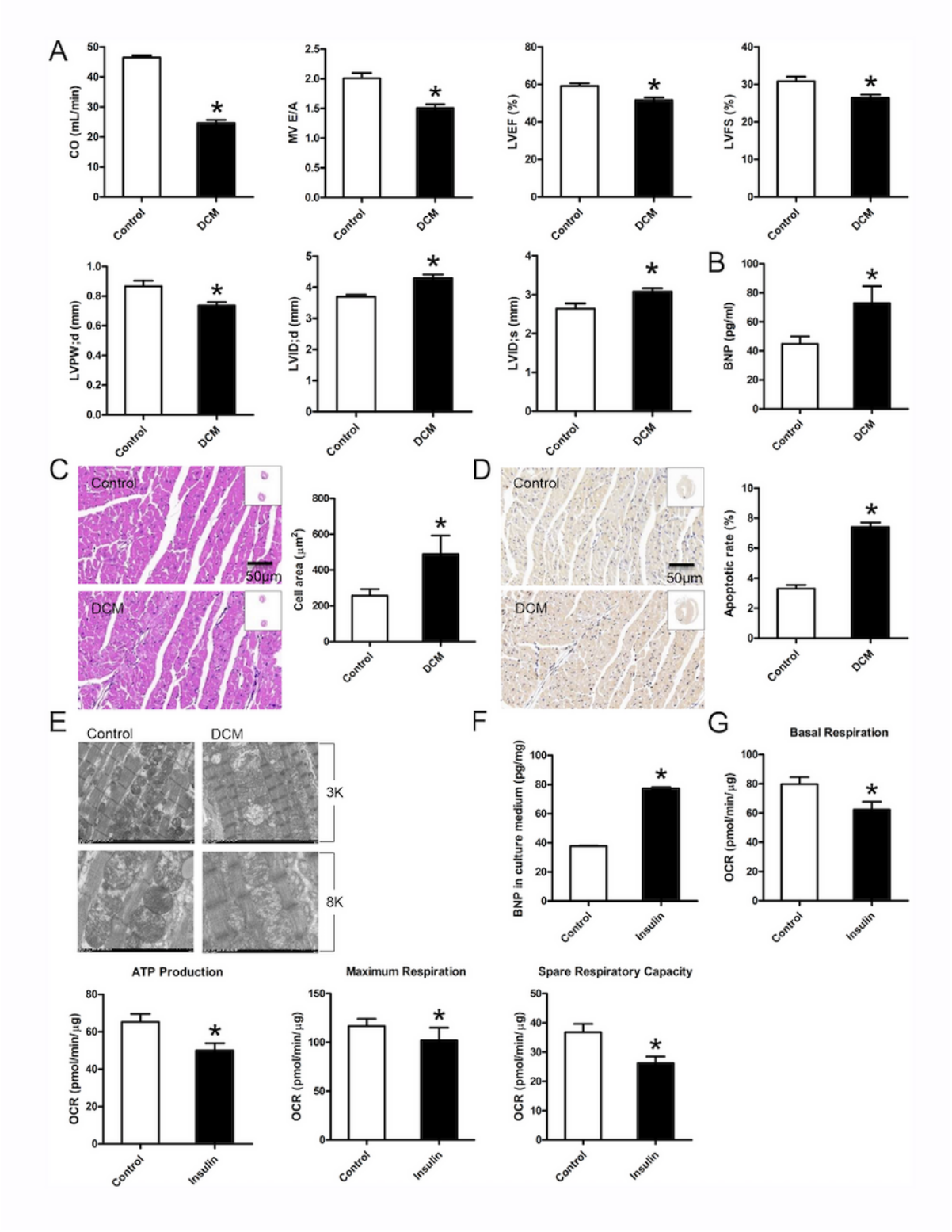

Figure 1

Cardiac and mitochondrial function are decreased in DCM mice and in insulin-resistant NRVMs. A, The cardiac function of mice was determined by echocardiography. CO, cardiac output; MV E/A, ratio of mitral valve E velocity to A velocity; LVEF, left ventricular ejection fraction; FS, fractional shortening; LVPW; d, left ventricular posterior wall at diastolic; LVID; d/s, left ventricular internal diameter at diastolic/systolic. B, Expression of brain natriuretic peptide (BNP) in the serum was analyzed by ELISA. C, Cardiac histology. Representative transverse section of left ventricle stained with hematoxylin and eosin (Scale bar = 50 μm). For quantification, cell area measurements were performed on similar sections, and 20 nucleated cells were randomly selected for measuring the mean cell area. D, Apoptosis was detected by the TUNEL assay. The number of apoptotic cells in similar sections was counted and is shown as a percentage. E, The ultrastructure of hearts was analyzed by electron microscopy. Representative images of hearts with original magnification of ×3k (3000) and ×8k (8000) are shown. F, BNP expression in the culture medium was analyzed by ELISA. G, Seahorse XFe96 Analyzer was used to test the mitochondrial function in NRVMs, including basal respiration, ATP production, maximal respiration, and spare respiratory capacity. OCR, oxygen consumption rate. Values are expressed as the mean ± SEM. N = 5. *P < 0.05 vs. control.

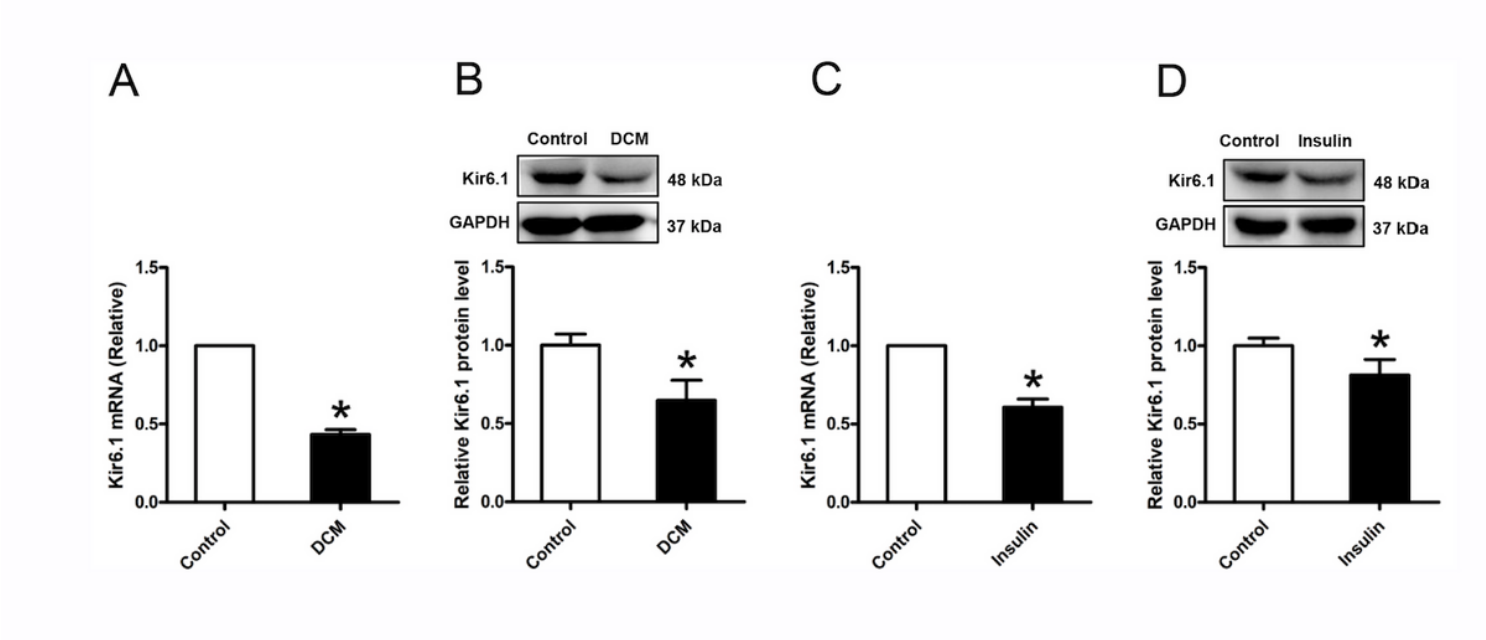

Figure 2

The expression of Kir6.1 is decreased in vivo and in vitro. Kir6.1 in HFD&STZ-induced type 2 diabetic mice and in chronic insulin-resistant NRVMs determined by qRT-PCR and western blotting. A, B, Kir6.1 in mouse cardiac tissue. C, D, Kir6.1 in NRVMs. Values are expressed as mean ± SEM. N = 5. *P < 0.05 vs. control.

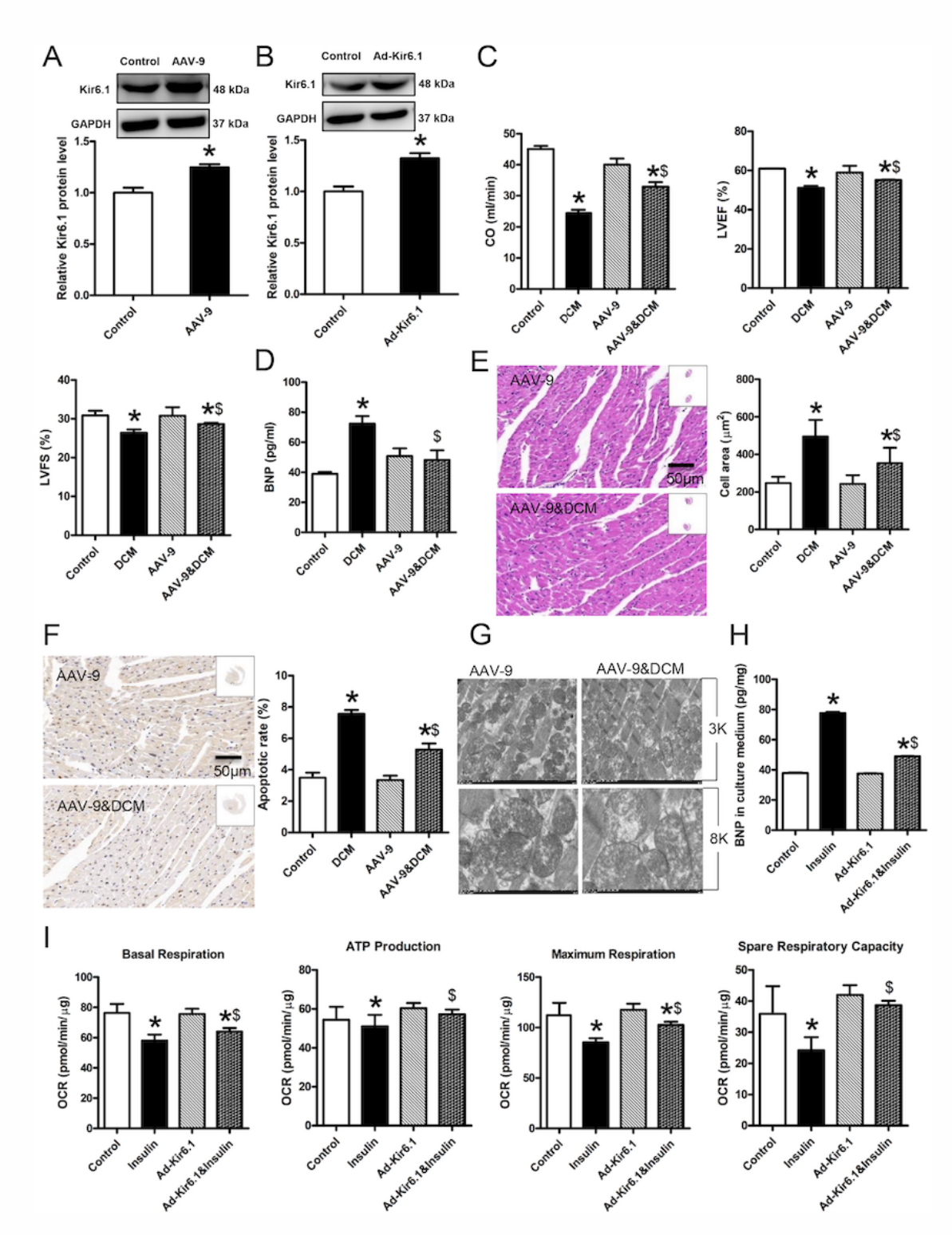

Figure 3

Kir6.1 overexpression improves cardiac dysfunction in DCM mice and in insulin-resistant NRVMs. A, Kir6. 1 expression in mice was confirmed by western blotting. Values are expressed as the mean ± SEM. N = 5. *P < 0.05 vs. control. B, Kir6.1 expression in NRVMs was confirmed by western blotting. Values are expressed as the mean ± SEM. N = 5. *P < 0.05 vs. control. C, Cardiac function in mice was determined by echocardiography. CO, cardiac output; LVEF, left ventricular ejection fraction; LVFS, left ventricular

fractional shortening. D, Brain natriuretic peptide (BNP) expression in the serum was analyzed by ELISA. E, Cardiac histology. Representative transverse section of left ventricle stained with hematoxylin and eosin (Scale bar = 50 μm). For quantification, cell area measurements were performed on similar sections, and 20 nucleated cells were randomly selected for measuring the mean cell area. Values are expressed as the mean ± SEM. *P < 0.05 vs. control; and $P < 0.05 vs. DCM. F, Apoptosis was detected by the TUNEL assay. The numbers of apoptotic cells in similar sections was counted and is shown as a percentage. *P < 0.05 vs. control; and $P < 0.05 vs. DCM. G, The ultrastructure of hearts was analyzed by electron microscopy. Representative images of hearts with original magnification of ×3k (3000) and ×8k (8000) are shown. H, The BNP expression in the culture medium was analyzed by ELISA. I, Seahorse XFe96 Analyzer was used to test the mitochondrial function in NRVMs, including basal respiration, ATP production, maximal respiration, and spare respiratory capacity. OCR, oxygen consumption rate. Values are expressed as the mean ± SEM. N = 5. *P < 0.05 vs. control; and $P < 0.05 vs. Insulin group.

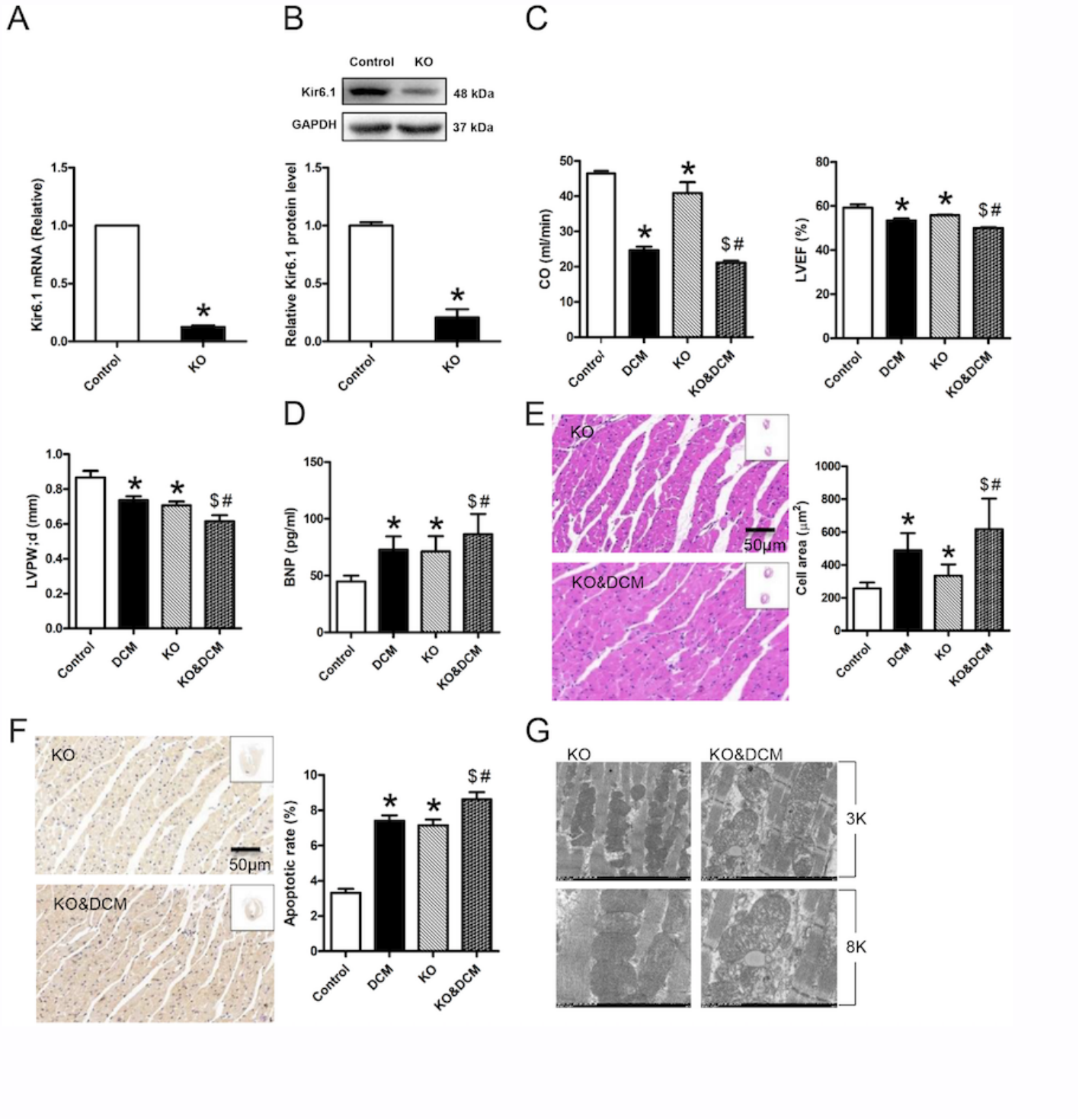

Figure 4

Cardiac-specific Kir6.1 knockout aggravates cardiac dysfunction in diabetic mice. A, The Kir6.1 mRNA expression in the heart of mice was examined by qRT-PCR. Values are expressed as the mean ± SEM. N = 5. *P < 0.05 vs. control. B, The Kir6.1 protein expression in the heart of mice was examined by western blot analysis. Values are expressed as the mean ± SEM. N = 5. *P < 0.05 vs. control. C, Mouse cardiac function was determined by echocardiography. CO, cardiac output; LVEF, left ventricular ejection fraction;

LVPW; d, left ventricular posterior wall thickness at diastole. Values are expressed as the mean ± SEM. N = 5. *P < 0.05 vs. control; and $P < 0.05 vs. DCM; #P < 0.05 vs. KO group. D, Brain natriuretic peptide (BNP) expression in the serum was analyzed by ELISA. Values are expressed as the mean ± SEM. N = 5. *P < 0.05 vs. control; and $P < 0.05 vs. DCM; #P < 0.05 vs. KO group. E, Cardiac histology. Representative transverse section of left ventricle stained with hematoxylin and eosin (Scale bar = 50 μm). For quantification, cell area measurements were performed on similar sections, and 20 nucleated cells were randomly selected to measure the mean cell area. Values are expressed as the mean ± SEM. *P < 0.05 vs. control; and $P < 0.05 vs DCM; #P < 0.05 vs. KO group. F, Apoptosis was detected by the TUNEL assay. The number of apoptotic cells in similar sections was counted and is shown as a percentage. *P < 0.05 vs. control; and $P < 0.05 vs. DCM; #P < 0.05 vs. KO group. G, The ultrastructure of hearts was analyzed by electron microscopy. Representative heart images with original magnification of ×3k (3000) and ×8k (8000) are shown.

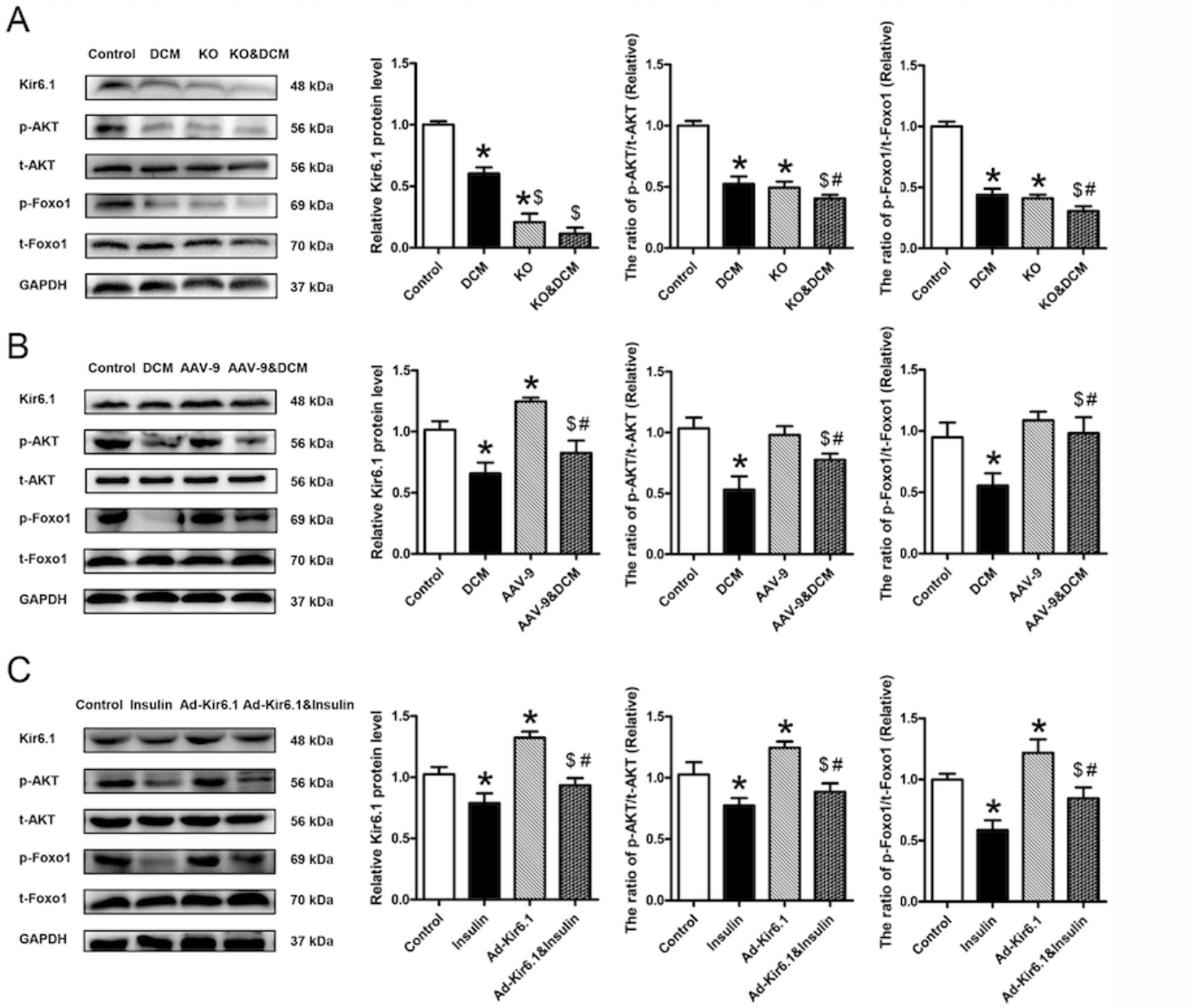

Figure 5

Effect of Kir6.1 on the AKT-Foxo1 signaling pathway in DCM. A, Western blotting was performed to quantify the expression levels of Kir6.1, p-AKT, and p-Foxo1 in the heart of mice. Values are expressed as the mean ± SEM. N = 5. *P < 0.05 vs. control; and $P < 0.05 vs. DCM; #P < 0.05 vs. KO group. B, Western blotting was performed to quantify the expression levels of Kir6.1, p-AKT, and p-Foxo1 in the heart of mice. Values are expressed as the mean ± SEM. N = 5. *P < 0.05 vs. control; and $P < 0.05 vs. DCM; #P < 0.05 vs. AAV-9 group. C, Western blotting was performed to quantify the expression levels of Kir6.1, p-AKT, and p-Foxo1 in NRVMs. Values are expressed as the mean ± SEM. N = 5. *P < 0.05 vs. control; and $P < 0.05 vs. Insulin group; #P < 0.05 vs. Ad-Kir6.1 group.

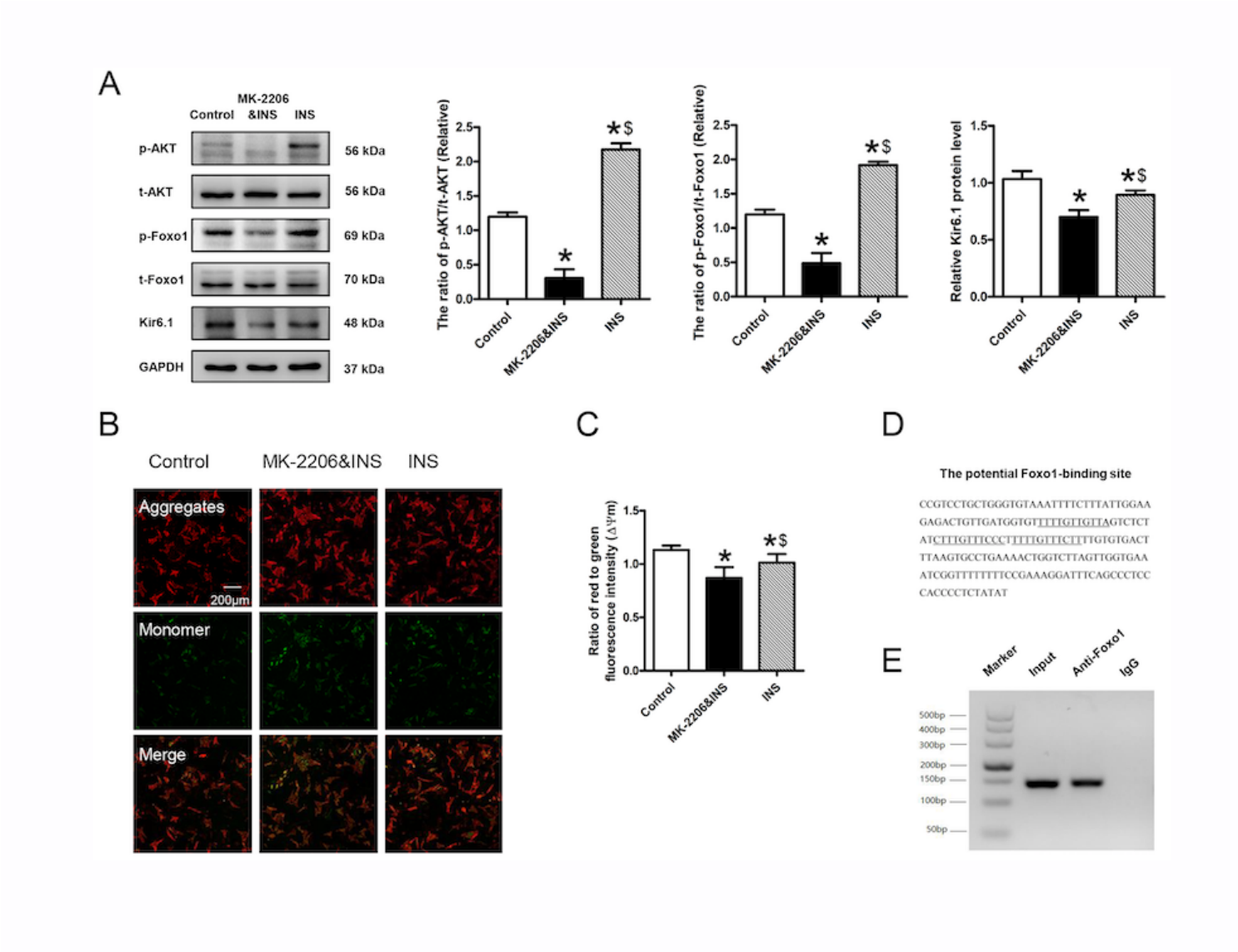

Figure 6

Effect of the AKT-Foxo1 signaling pathway in regulating Kir6.1 expression and mitochondrial function in cardiomyocytes. A, Western blotting was performed to quantify the expression levels of Kir6.1, p-AKT, and p-Foxo1 in cardiomyocytes. Values are expressed as the mean ± SEM. N = 5. *P < 0.05 vs. control; and $P < 0.05 vs. MK-2206&INS. B, Determination of ΔΨm in the three groups of cardiomyocytes by the fluorescent dye, JC-1 (Scale bar = 200 μm). C, Comparison of the ΔΨm among the three groups of cardiomyocytes. For quantification, 20 cells were randomly selected to calculate the ΔΨm levels by comparing red fluorescent intensity to green fluorescent intensity. Values are expressed as the mean ± SEM. *P < 0.05 vs. control; and $P < 0.05 vs. MK-2206&INS. D, Potential Foxo1-binding sites are located 2.0 kb upstream of the Kir6.1 gene's transcription initiation site. E, Binding of endogenous Foxo1 from the hearts of mice to the potential Foxo1-binding site was confirmed by the chromatin immunoprecipitation assay. Representative results from three independent experiments are shown.

Supplementary Files

This is a list of supplementary files associated with this preprint. Click to download.

- supplement1.docx